Heliyon 9 (2023) e22363

Contents lists available at ScienceDirect

Heliyon

journal homepage: www.cell.com/heliyon

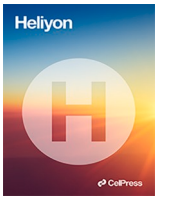

Demonstration of the stabilization of solar salt at 620 C with a semi-closed configuration in a 100 kg-scale

Sebastian Kunkel [a,*], Felix Seeliger [b], Andrea Hanke [a], Thomas Bauer [b], Alexander Bonk [a]

[a] German Aerospace Center (DLR), Institute of Engineering Thermodynamics, 70569, Stuttgart, Germany
[b] German Aerospace Center (DLR), Institute of Engineering Thermodynamics, 51147, Cologne, Germany

ARTICLE INFO

Keywords:
Thermal stability
Nitrate salt
molten salt
High temperature chemistry
Technical-scale chemistry

ABSTRACT

Among the variety of energy storage techniques thermal energy storage (TES), based on molten salts, is already in use for the storage of heat in a gigawatt hour scale. At the time of writing virtually all TES in CSP utilize Solar Salt (60 wt-% $NaNO_3$ and 40 wt-% KNO_3) due to its competitively low price, low vapor pressure and non-toxicity. On the downside, the operating temperature is limited to 560 °C based on its thermal stability. However, increasing the operating temperature while maintaining thermal stability of the salt using techniques that are realizable in industrial scale remains one of the main challenges. Up to now this could only be achieved in a small scale by flushing with synthetic purge gas or sealing and pressurizing the system, maintaining the necessary gas atmosphere and shifting the chemical equilibrium to the nitrate side. Both methods are hardly realizable in an industrial scale. In this work we show a new strategy to stabilize Solar Salt at 620 °C by combining the gas-purged configuration and sealed system with maximum pressure of few tens of millibars in a 100 kg scale. The formed gas phase was within the expected range in terms of oxygen and nitrous gases. Additionally, the concentration of the nitrate and nitrite ions aligned well with salt systems with gas-purged atmosphere at 620 °C. We demonstrate the first experiments on long-term thermal stabilization (4000 h) of Solar Salt at 620 °C in a 100 kg technical-scale. These findings represent an important step in the development of modern storage systems.

1. Introduction

Today thermal energy storage (TES) plays a crucial role for the efficient use of green, renewable and sustainable energy sources [1]. In this field a distinction between different TES systems can be made: thermochemical heat, latent heat and sensible heat. Systems referring to thermochemical heat are using reversible chemical reactions. The heat is stored during an endothermic reaction and released via an exothermic reaction. One important example is the system $CaO/Ca(OH)_2$ with water as a reactant. Latent systems utilize phase transitions (e.g. solid to liquid) of phase change materials (PCMs) to store energy. Lastly, the sensible heat storage systems are using the heat capacity of materials with different states of aggregation (e.g. solid: ceramics, liquid: molten salt) to store thermal energy during a temperature change [2]. Molten nitrate salts are promising materials in the field of TES as well as heat transfer fluids (HTS) and are already in use with temperatures up to 560 °C. Especially for the sensible heat storage system, molten nitrate salts based

* Corresponding author.
E-mail address: Sebastian.kunkel@dlr.de (S. Kunkel).

https://doi.org/10.1016/j.heliyon.2023.e22363
Received 30 May 2023; Received in revised form 31 October 2023; Accepted 10 November 2023
Available online 23 November 2023

on alkaline and alkaline earth metals are used. The most common one is a mixture of 60 wt-% $NaNO_3$ and 40 wt-% KNO_3, known by the name Solar Salt [3]. Currently this kind of salt mixture is used at up to 560 °C storage temperature under air atmosphere and atmospheric pressure of the tank in power plants like the *Cerro Dominador* in Chile with a storage capacity of 110 MW [4–10].

The limitation of the operating temperature can directly be connected to the stability of the nitrate ion (NO_3^-) in terms of decomposition and consequent changes of the salt's thermodynamic properties as well as corrosivity towards the structural materials [7,11–16]. It is well established that the nitrate ion is decomposing with a reversible reaction, according to reaction (1) to nitrite ions (NO_2^-) and oxygen (O_2). Thereby, the chemical equilibrium is strongly depending on the temperature and the oxygen partial pressure. Furthermore, an ongoing decomposition of the nitrite ion to nitrous gases (e.g. NO, NO_2) and dissolved oxide ions (e.g. O^{2-}, O_2^-, O_2^{2-}) takes places, as can be seen in reaction (2). Despite the fact that reaction (2) is widely accepted, the exact stoichiometry has not been verified yet and other reaction paths might be favored at different temperatures and gas compositions [12,17,18].

$$NO_{3(l)}^- \rightleftharpoons NO_{2(l)}^- + 0.5\ O_{2(g)} \quad (1)$$

$$NO_{2(l)}^- \rightleftharpoons NO_{(g)} + NO_{2(g)} + O_{(l)}^{2-} \quad (2)$$

in recent years, experiments in a laboratory scale (≤150 g) showed the possibility of stabilizing molten Solar Salt at elevated temperatures up to 620 °C either by purging the gas atmosphere with reactive gases (NO_x and O_2) or by closing the system and conserving the evolving gases under pressure build-up inside the system [19,20].

In this work we present the first experiments with Solar Salt at 620 °C in a technical lab scale (100 kg) utilizing a combination of a gas-purged and closed system, later defined as "semi-closed" system, as a new way to stabilize Solar Salt at elevated temperatures up to 620 °C under application of relevant conditions ($p_{max} = 20$ mbar overpressure) over 4000 h storage time. During the course of this first of its kind experiments the salt chemistry is analyzed in terms of the anion composition ($NO_3^-/NO_2^-/O^{2-}$), while the composition ($NO/NO_2/O_2/CO_2$) of the gas phase inside the reactor is measured with a connected gas analyzing system. With this method, this paper outlines for the first time that Solar Salt can be operated and stabilizes at 620 °C in a 100 kg scale for 4000 h in a semi-open system at ambient pressure beyond the state of the art in science and technology.

2. Experimental section

The experiments were performed in a steel vessel with basket bottom (Material: 2.4816 steel, volume 134 L), placed and heated within a circular four-zone gradient furnace (Carbolite Gero GmbH & Co. KG, Germany) as shown in Fig. 1. The steel vessel was gas-sealed with a top flange and mica flat gasket. Six weld-on pipe sockets were used for different thermocouples (type K, class 1), pressure control (mechanical overflow valve), a mechanical stirrer, a salt sampling system as well as gas inlet and outlet. In front of the latter, interconnected metal shields are installed to minimize salt evaporation and heat radiating to the outgoing gas analyzing system. Due to unheated installations at the upper part of the retort a temperature gradient developed, resulting in natural convection inside the molten Solar Salt volume. This natural convection has helped to prevent temperature stratification in the molten salt. Additionally, a build-in axial stirrer (Material: 2.4819 Hastelloy C-276 steel) was used for homogenizing the melt. The gas inlet can be operated in two ways, either purging the gas phase above the salt melt or bubbling the reactive gas through the liquid phase. A modular gas analysis system is integrated into the gas control system which was optionally used or bypassed as needed. Switching between a permanent and non-permanent gas measuring routine via valve Va4 and valve Va5 was realized in order to save the gas analysis from prolonged

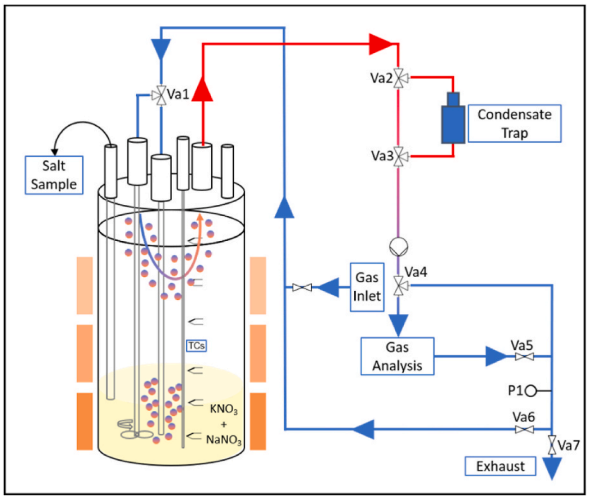

Fig. 1. Scheme of the 100 kg technical-scale test rig at DLR cologne. The two-colored globules emphasize the different possibilities of gas flow, either purging the gas phase above the salt melt or bubbling gas through the liquid phase.

exposure to corrosive sample gas. With two valves (Va6 and Va7) and a pressure sensor (P1) behind the gas analyzing system, it was possible to operate the system in two different configurations. The pressure sensor (P1) configured to measure the pressure relative to the local atmospheric pressure up to a maximum of 20 mbar overpressure. When this limit is exceeded, Va7 opens to regulate the pressure down.

1.) a **semi-closed configuration**, cycling the gas phase with support of a pump through the system (p_{max} = 20 mbar overpressure, Va6 open, Va7 open when p (P1) > 20 mbar, see Fig. 1)
2.) **open configuration** by releasing accumulated gases through an exhaust pipe (Va6 closed, Va7 permanent open, see Fig. 1).

The molten salt experiments were performed with a combination of an open and a semi-closed configuration. Fig. 2 schematically shows the course of the three experiments presented in this study. In the open configuration gas was purged above the melt with atmospheric pressure, whereas during the semi-closed configuration no gas was purged, but the gas atmosphere was cycled within the system while maintaining a maximum overpressure of 20 mbar inside the whole system. The initial salt mixture for the **first experiment (V1)** was produced by mixing 93,5 mol-% Solar Salt (64 mol-% $NaNO_3$, 36 mol-% KNO_3, refined grade, SQM Iodine, Spain) with 6,5 mol-% $NaNO_2$ (refined grade, Bernd Kraft, Germany) directly inside the retort. Starting with a specific amount of nitrite salt in the initial salt mixture instead of using pure Solar Salt was expected in order to lower the thermal decomposition of the salt by equation (1) and reducing the time to reach an equilibrium at 560 °C. Melting, homogenizing and dehumidifying of the salt was performed at 300 °C for 240 h while purging the atmosphere above the melt with dry nitrogen gas (0.2 L/min gas flow). The dried salt was heated up to 560 °C in the open configuration with a synthetic air gas flow of 4 L/min. After isothermal heating of 240 h the system was changed to the semi-closed configuration with no purge gas, heated up to 620 °C and the temperature was again kept constant for 1500 h. In order to archive a constant temperature over a long time, the temperature of the salt was constantly measured and maintained by heating with the four-zone gradient furnace. At the end of the isotherm, the system was cooled down to 300 °C under synthetic air flow in order to bleed the system and finish the experiment. To prevent a solidification of the salt between the experiments the salt temperature was held constant at 300 °C.

For the **second experiment (V2)** the salt from the first experiment was reused in order to investigate the cycle behavior in the 100 kg scale. Additionally, an axial conveying stirrer was used, varying the stirring speed from 250 rpm to 0 rpm in two steps (500 h per step) in order to test the behavior of an already decomposed salt while simulating convection effects. At the end of V2 again the system was switched to the open configuration and purged with a gas flow of 0.5–1 L/min (50 vol-% O_2, 50 vol-% N_2 and 2000 ppm NO) in order to regenerate a fraction of Nitrite/Oxide ions over 400 h (in the following mentioned as **Regeneration study V3**) [17]. Subsequently, the salt was cooled down to room temperature under nitrogen gas flow to finish the experiment.

During the course of each experiment, in-situ gas analysis measurements (6 data points per minute) were carried out simultaneously using an AO2000 system (ABB Automation GmbH, Germany) equipped with three optical detectors for NO (Limas11, 0–10,000 ppm ±0.5 %), NO_2 (Limas11, 0–10,000 ppm ±0.5 %; Uras26, 0–10,000 ppm ±0.4 %) and O_2 (Magnos206, 0–100 vol-% ± 0.5 %). Additionally, salt samples were taken from the reaction vessel four times per week. For this purpose, corundum crucibles attached to a stainless-steel chain (well-bucket sampling method) were dropped inside the salt through one of the unused weld-on pipe sockets until touching the bottom of the steel vessel. By pulling out the chain and crucible a representative salt sample was obtained and subsequently analyzed to quantify the content of nitrate, nitrite and oxide ions. The amount of the nitrate and nitrite ions were analyzed by ion-exchange chromatography (IC) using an 883 Basic IC plus (Metrohm AG, Switzerland) equipped with a Metrosep A

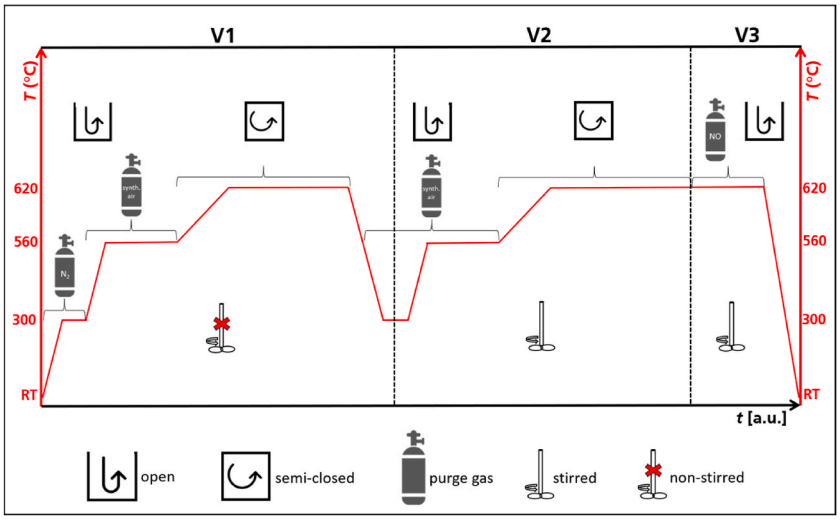

Fig. 2. Principle diagram of the three experiments discussed in this study, emphasizing the applied temperature, configuration, purged gas and stirrer mode.

Supp analytical column (5 × 250 mm) and a suppressed conductivity detector. The oxide ion concentration measurement was done with a potentiometric controlled acid-base neutralization titration apparatus (Metrohm Titrando 905, Metrohm AG, Switzerland) with an 0.01 M aqueous HCl solution and equipped with automatic dosing units, Metrohm 800 Dosino. The procedures for the salt analyses are described in more detail by Bonk et al. [13].

3. Results and discussion

Different strategies to avoid the decomposition of Solar Salt according to equations (1) and (2) under formation of high nitrite and oxide ion levels are known. The most common one is the application of a purge gas which contains high levels of nitrous gases and oxygen resulting in a shift of the chemical equilibrium and thereby a reduction of nitrite and oxide levels in the melt. On the downside, large amounts of toxic and reactive gases must be stored and handled. This, in conjunction with the gas consumption, adds to the costs and the safety requirements of this method. Alternatively, the whole system can be operated as a closed system, conserving the gas phase formed during decomposition, also pushing the equilibrium to the nitrate and nitrite side. This approach goes side by side with a considerably high pressure increase in the whole system, while only a few tens of millibar are acceptable in a large scale flat-bottom tanks, typically used for 2-tank molten salt storage. To overcome these problems the two stabilization experiments on Solar Salt at 620 °C in a 100 kg scale were performed with a combination of an open configuration ($T = 25 - 560$ °C, 4 L/min synth. air purge gas) and closed configuration ($T = 560 - 620$ °C, $p_{max} = 20$ mbar), hereinafter entitled as semi-closed configuration. Additionally, to prevent decomposition and high oxygen development at 560 °C, 6.5 mol-% Nitrite was added to the initial salt mixture. In the following, two experiments (V1 and V2) are shown and discussed. The results of both experiments are compared to published lab-scale experiments from Sötz et al. performed in a purged system in a mg- and g-scale with respect to the chemical equilibrium and with experiments in a small 1.5 g scale for comparison of the kinetic behavior to identify similarities and up-scaling effects [20–22]. Additionally, a short study (V3) on the regeneration of the degenerated and decomposed Solar Salt remaining after both experiments was performed and discussed in the chapter Regeneration.

3.1. Stabilization experiments V1 and V2

The obtained sets of data from both stabilization experiments under applying the semi-closed configuration are shown in Figs. 3 and 4. In both experiments V1 and V2 an increase of oxygen concentration in the gas phase over the molten salt up to about 60 vol-% can be detected after closing the system (Fig. 3, left). The delayed increase in the **first experiment** results from an operational error and accidental dilution of the gas phase with atmospheric air inside the system. Ongoing dilution or bigger leakage can be excluded, since no additional CO_2 was found in the gas analysis data. After reaching the peak concentration, the O_2 concentration decreases steadily over time until the end of the experiment. Molten salt analysis shows, that the nitrite concentrations are very stable during the isotherm at 560 °C within the first 400 h. After heating to 620 °C and semi-closing the system, the nitrite levels increase almost linearly between 400 h and 800 h from 6.25 mol-% to 8.25 mol-%. After that, the rate of nitrite formation decreases but remains relatively steady till the end of experiment V1 after 1700 h, with a final nitrite concentration of 9.6 mol-%. From the quantity of molten salt and the level of nitrite formed, the quantity of evolved oxygen according to Eq. (1) while maintaining the maximum overpressure of 20 mbar can be calculated. This calculation shows, that the quantity of released oxygen should result in O_2 concentrations at or above 90 vol-%, which is much higher than the levels detected in the experiment. Cooling down to 300 °C while purging the gas phase with nitrogen gas results in a slight decrease of the nitrite concentration from 9.6 mol-% to 9.4 mol-%.

After starting the second experiment, using the open configuration, the O_2 concentration showed the same behavior, peaking up to roughly 60 vol-% and subsequently decreasing steadily over time until the end of the experiment. The salt analysis shows a decrease in nitrite content from the initial 9.4 mol-% to 8.27 mol-% during the isotherm at 560 °C. After applying the semi-closed configuration

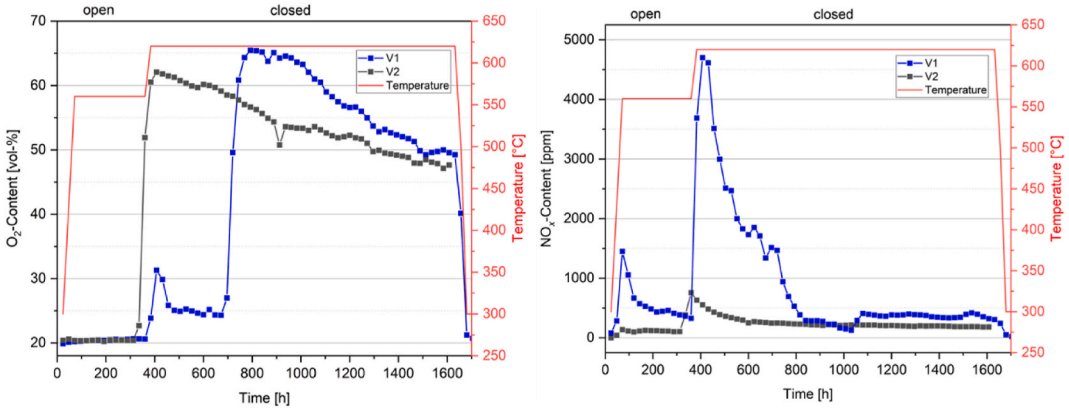

Fig. 3. Oxygen (left) and nitrous gas ($NO + NO_2$, right) concentrations and temperatures recorded during the course of the stabilization experiments V1 (blue) and V2 (black). Each data point corresponds to the average of all data points in a duration of 24 h.

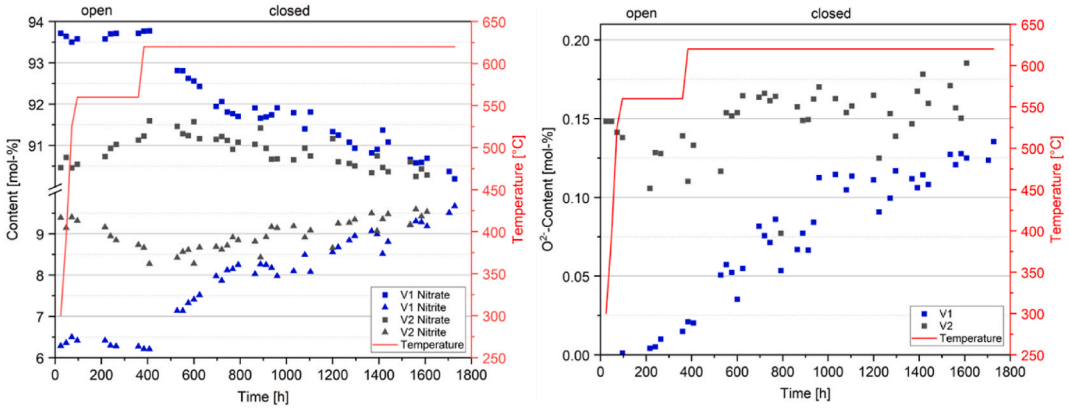

Fig. 4. Content of temperatures (left + right), nitrate and nitrite ions (left) as well as oxide ions (right) of the salt melts of both 100 kg scale stabilization experiments V1 (blue) and V2 (black).

while heating to 620 °C the nitrite level again increases between 400 h and 1400 h from 8.27 mol-% to 9.5 mol-%. After that the nitrite concentration remains relatively steady till the end of experiment V2 after 1600 h, with a final nitrite concentration of 9.5 mol-%. Once again, the measured quantity of released oxygen distinctly differs from calculated concentration.

Molten salt analysis shows, that the initial salt mixture in the **first experiment** features no significant changes in nitrate and nitrite ion content during the isotherm at 560 °C, indicating that reaction (1) already reached equilibrium. After closing the system and heating to 620 °C an ongoing thermal decomposition of the nitrate to nitrite and oxygen occurs until again the chemical equilibrium is almost reached. Extrapolation of data leads to a nitrite concentration of about $X_{\mathrm{Nitrite}} \approx 10$ mol-%. In contrast, in the **second experiment** the aged salt partially regenerates during the isotherm at 560 °C shifting the equilibrium back to the nitrate side. The nitrate concentration decreased by ≈ 1.5 mol from 9.4 mol-% (0 h) to 8.27 mol-% (400 h). Subsequent closing and heating of the system to 620 °C leads to an ongoing decomposition under an increase of nitrite with values from 8.27 mol-% (400 h) to 9.5 molt% (1600 h).

As already mentioned, both experiments exhibit a maximum oxygen concentration of around 60 vol-%. However, from the amount of nitrite formed due to the beforehand mentioned ongoing thermal decomposition of the salt after semi-closing the system (≈1.5 mol-%, Fig. 4, left) and according to reaction (1), a steady accumulation of oxygen in the gas phase, while maintaining a maximum overpressure of 20 mbar, with a final concentration at up or above 90 vol-% is expected. Additionally, over the course of around 1000 h both experiments show a steady decrease to 50 vol-% O_2. One possible reason for these differences is a high temperature corrosion reaction of the hot steel surface of the vessel with oxygen, either from the gas phase or dissolved in the molten salt. For this consideration 15 μm were used as typical thickness of the corrosion layer on Alloy 600 after 1700 h reaction time, but are prone to errors since it is biased by the unknown surface structure/area of the corroded steel surface, changing salt composition and local impurity concentrations. Measured against the chromium and iron content of the used steel (Cr: 14–17 %, Fe: 6–10 %), a corrosion layer of ≤15 μm, would already be sufficient to compensate for both, the lower oxygen concentration during the decomposition of the salt after closing of the salt after closing the system, as well as the loss of 10 vol-% oxygen during the subsequent 1000 h. An assumed incipiently rapid absorption and reaction of oxygen with the steel surface, which progresses more slowly over time, corresponds to the corrosion behavior of the used type of steel described in literature (2.4816/Alloy 600) [23,24]. The rough surface of the reaction vessel, caused by previous cleaning before starting the experiments, additionally enhances the corrosive reactions. However, in order to confirm this theory, corrosion specimens would have to be extracted from the vessel which was not part of this study.

The measurements of nitrous gases are shown in Fig. 3 (right). **The first experiment** features a short increase in concentration ($X_{\mathrm{NOx,\,max}} \approx 1500$ ppm) after heating up to 560 °C with subsequent downward drift. When heating up to 620 °C and applying the semi-closed configuration larger increase of NO_x ($X_{\mathrm{NOx,\,max}} \approx 4500$ ppm) could be measured. After reaching the peak concentration, the NO_x concentration decreases steadily over time until the end of the experiment V1 resulting in a final plateau at around 350 ppm. The molten salt analysis shows, that the oxide ion concentration is very stable during the first 200 h of the isotherm at 560 °C. During 200 h and 400 h a distinct increase could be observed. After heating to 620 °C and semi-closing the system, the oxide levels increase almost linearly until 800 h. From 800 h till the end of experiment V1 at 1700 h the oxide concentration increases slightly lower, with a final oxide concentration of 0.14 mol-%. It needs to be emphasized that a clear spread in the measurement data can be observed at 620 °C salt temperature. After cooling down to 300 °C while purging the gas phase with nitrogen no NO_x could be measured. The **second experiment** again features a steady NO_x concentration of around 120 ppm after heating the system to 560 °C holding the temperature isothermal for 300 h. After heating up to 620 °C V2 showed a peak in the NO_x concentration ($X_{\mathrm{NOx,\,max}} \approx 750$ ppm) that is subsequently decreasing steadily between during the isotherm at 560 °C. After heating to 620 °C the oxide concentration again increases between 400 h and 700 h up to 0.17 mol-%. After that the oxide level remains relatively constant till the end of experiment V2 after 1600 h, with a final oxide ion concentration of 0.17 mol-%.

The salt composition data for oxide ions obtained by ion chromatography for the **first experiment** features no significant changes during the beginning 200 h of the isotherm at 560 °C since the thermal decomposition according reaction (2) occurs relatively slow,

resulting in oxide concentrations below the analytical measurement minimum. For that reason, the observed amount of NO_x during the first 100 has to be the result of a decomposition of small amounts of magnesium nitrate $Mg(NO_3)_2$ to MgO and nitrous gases, according to equation (3). Magnesium nitrate is a typical impurity in non-synthetic Solar Salt. Additionally, a formation of NO_x due to nitrite decomposition would lead to an increase of the oxygen concentration, which is not observable in the obtained data in the first 100 h.

$$2\ Mg(NO_3)_2 \rightleftharpoons 2\ MgO + 4\ NO_2 + O_2 \tag{3}$$

The continouse formation of nitrous gases in combination with the slow increase of oxide concentration during the next 200 h of the isotherm at 560 °C arise from a beginning thermal decomposition of the nitrite ions according to equation (2). After heating to 620 °C and semi-closing the system, the oxide levels increase almost linearly until 800 h while the gas analysis measurement simultaneously display a strong increase of NO_x ($X_{NOx,\ max} \approx 4500$ ppm) at around 400 h with subsequent downward drift and a plateau at around 300 ppm NO_x. This peak is ascribed to the oxidation of the steel surface by the molten salt which generally is accompanied by the formation of nitrous gases, as e.g. shown in Brough's work [25]. The ongoing, albeit slower, formation of oxide ions accompanied by a constant NO_x emission after 800 h reaction time can presumably be explained by a nonequilibrium between the big salt volume and the gas phase in the reactor. For the next 800 h till the end of the **first experiment** the oxide ion content exhibits a steady increase up to $X_{Oxide} \approx 0.14$ mol-%, that can be described by the ongoing thermal decomposition according to equation (2). The permanent formation of nitrous gases supports this hypothesis.

In contrast, in the **second experiment** the aged salt shows a small decrease in oxide content from 0.14 mol-% to 0.13 mol-% during the isotherm at 560 °C, which is a result from a staring regeneration, shifting the equilibrium in equation (2) to the nitrite side. The constant emission of 120 ppm NO_x during that time can presumably be explained by the beforehand mentioned non-equilibrium between salt and gas phase or the ongoing corrosion of the steel surface under formation of nitrous gases. After heating to 620 °C and applying the semi-closed configuration the gas analysis measurement emphasizes a similar behavior compared to the first experiment showing a NO_x peak with subsequent decrease between a steady emission of 200 ppm till the end of experiment V2. That peak directly after closing the system can be ascribed to corrosion reactions as well as the still ongoing setting of the chemical equilibrium according equation (2). As expected, the oxide concentration also increases between 400 h and 700 h up to 0.17 mol-%. After that the oxide level remains relatively constant till the end of the **second experiment** after 1600 h, with a final oxide ion concentration of 0.17 mol-% emphasizing that an equilibrium according equation (2) is almost reached.

In general, from the gas and salt analysis measurements it is clearly evident, that by closing the system and conserving the formed oxygen and nitrous gases in the gas phase using the semi-closed configuration the chemical equilibrium of equation (1) is shifted to the nitrate side. The relatively constant oxide concentration at the end of the second experiment indicates, that, despite having high final oxide ion concentrations, an equilibrium for equation (2) was also archived. Although the second experiment was performed while varying the speed of the stirrer, no direct correlation between the speed and the salt chemistry could be found.

3.2. Equilibrium

3.2.1. Nitrate/nitrite

For a better comparability of the data, the concentrations of nitrate and nitrite as well as oxygen partial pressures for further calculations are evaluated at the end of each temperature step (560 °C and 620 °C) for both experiments. With those values the reaction quotient Q is calculated, according to equation (4). Due to purging of the system with synthetic air and comparably low formation of oxygen during the decomposition of the nitrate, according to equation (1), the partial pressure of oxygen p_{atm,O_2} was estimated as constant 0.2 atm at 560 °C. For 620 °C the oxygen concentration measured with the gas atmosphere at the end of the experiment ($p_{atm,O_2} = 0.5$ atm) was used as the partial pressure of oxygen. When an equilibrium is reached, Q equals the equilibrium constant K (see equation (5)). Hereinafter, for simplification K instead of Q is used in the further discussion of the data.

$$Q_N = \frac{[NO_2^-]}{[NO_3^-]} \cdot p_{O_2}^{0.5} \tag{4}$$

Table 1
Oxygen partial pressures, nitrite/nitrate ratios and equilibrium constants from experiments of this study and reference data.

Temperature [°C]	p_{O_2}	$\frac{[NO_2^-]}{[NO_3^-]}$ [mol•mol^{-1}]	ln$K$	Reference
475	0.2	0.0229	−5.6351	Sötz et al. [21]
500	0.2	0.0198	−4.8704	Sötz et al. [21]
525	0.2	0.0178	−4.3677	Sötz et al. [21]
550	0.2	0.0168	−4.1420	Sötz et al. [21]
560	0.2	0.0669	−3.5094	V1, this study
	0.2	0.0903	−3.2092	V2, this study
600	0.2	0.1120	−2.9955	Sötz et al. [20]
620	0.2	0.1560	−2.6624	Sötz et al. [20]
	0.5	0.1052	−2.5983	V1, this study
	0.5	0.1063	−2.5881	V2, this study

$$K_N = \lim_{t\to\infty} Q_N \tag{5}$$

The obtained nitrite/nitrate ratios and calculated equilibrium constants of this 100 kg study and published data from lab scale experiments (≤100 g) are summarized in Table 1 and compared in a van't Hoff plot (see Fig. 5).

The values of ln$K$ for equation (1) at 620 °C of both 100 kg experiments V1 and V2 align well within the uncertainty areas set by linear fit through work by Sötz et al. (mg- and 100 g-scale) but are shifted to higher ln$K$ at 560 °C (Fig. 5) [20,21]. Those shifts can be ascribed to different reasons. The most likely one is the less ideal experimental conditions of a technical scale test rig compared to a laboratory set up. The molten salt in 100 kg was exposed to a larger steel surface area (retort, stirrer) compared to the lab-scale, which cause a high nitrite formation, and thus oxide ion formation as can be seen in Fig. 4 (right). This corrosion driven salt decomposition, as described by equation (6) in Brough's work, results in an increase of the salts nitrite level and subsequently a higher nitrite-nitrate-ratio and thus a higher ln$K$ [25].

$$2\ Cr + 7\ NO_3^- \rightleftharpoons Cr_2O_7^{2-} + 5\ NO_2^- + 2\ NO_2 \tag{6}$$

in case of V2 the aged Solar Salt additionally underwent an uncomplete regeneration reaction at 560 °C, whereas the previous experiment V1 was stopped before an equilibrium was reached resulting in higher nitrite values as expected.

According to these findings it becomes clear, that on a 100 kg scale at 620 °C a nitrite-nitrate equilibrium constant, which agrees with the already published equilibrium constants from laboratory experiments was obtained. In contrary to these 100 g scale experiments that were performed with an open system, on the 100 kg scale a semi-closed system was applied, which led to an accumulation of the oxygen partial pressure (approx. 0.5 bar) compared to the laboratory experiment (0.2 bar). The absolute pressures were almost identical in the laboratory and 100 kg experiments (roughly atmospheric pressure). Also, it is shown, that when the system is closed, a maximum pressure increase of ≈20 mbar is sufficient to accumulate enough oxygen in the atmosphere to stabilize the salt in relation to the nitrite content, maintaining a salt composition which might still be useable in industrial scale tanks without strong corrosion.

3.2.2. Nitrite/oxide

As can be seen in Fig. 6, the change of the oxide content became very low after 700 h of testing, indicating that an oxide ion equilibrium was attained for experiment V2. The considerable low reaction constant k_2 ($3.22 \bullet 10^{-12}\ s^{-1}$), shown in Table 2 support this hypothesis. A complete description of the equilibrium constant K, as previously shown for the Nitrate-nitrite-equilibrium is not possible, due to a lack of data in this study and literature. For that reason, further experiments focusing on the nitrite-oxide equilibrium are needed. Since permanent increasing oxide concentrations might lead to an increasing corrosion, maintaining a constant oxide concentration is one of the most important factors in terms of salt composition.

3.2.3. Kinetic

For the evaluation of up-scaling effects not alone stabilization of the molten salt but also the consideration of the reaction kinetics, formation rates of decomposition products, play an important role. These can be described by the reaction rate $r_{1/2}$ and reaction constants k_1 and k_2 of the reduction of equations (1) and (2) at 560/620 °C. Here, similar to various other kinetic studies, the decomposition reactions were approximated with a first order rate law and equation (7) for the nitrate-nitrite and equation (8) for the nitrite-oxide decomposition [22,26,27].

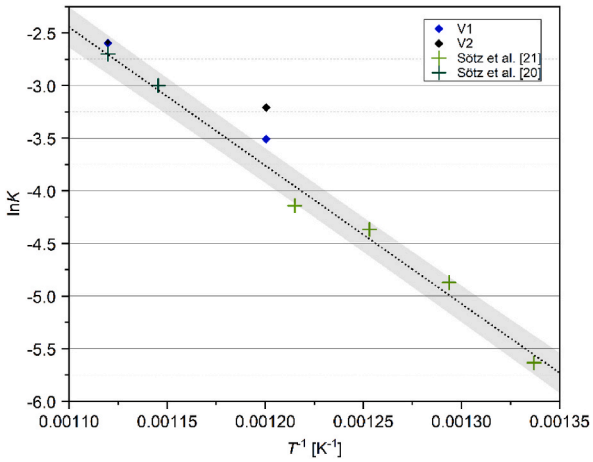

Fig. 5. Van't Hoff plots of the logarithmic equilibrium constants of equation (1). The rhombus symbols (black, blue) correspond to the equilibrium constants calculated in this study at 560 and 620 °C. For comparison, equilibrium constants (green cross symbols), their linear fit (dotted line) and the uncertainty range from previously published lab-scale mg-/g-scale studies are inserted [20,21].

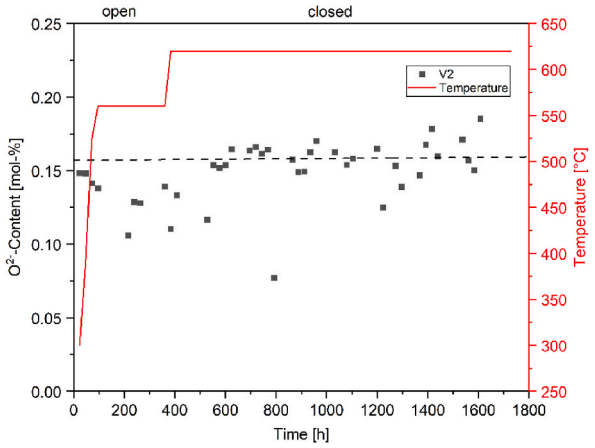

Fig. 6. Oxide ion concentration of experiments V2 (black squares) and linear fit of the data points (dotted line), emphasizing the small change in concentration over the course of the experiment.

Table 2
Reaction constants of the decomposition equations (1) and (2) determined in this study compared to previously published data obtained in lab scale experiments for $T = 560$ and 620 °C.

	Versuch 1		Versuch 2		Sötz et al. [21,22]	
Temperatur	560 °C	620 °C	560 °C	620 °C	560 °C	620 °C
k_1, Nitrate → Nitrite [s^{-1}]	–	$6.28 \bullet 10^{-09}$	–	$2.63 \bullet 10^{-09}$	$5.33 \bullet 10^{-06}$	$2.38 \bullet 10^{-05}$
k_2, Nitrite → Oxide [s^{-1}]	$3.19 \bullet 10^{-09}$	$1.82 \bullet 10^{-09}$	$2.26 \bullet 10^{-09}$	$3.22 \bullet 10^{-12}$	$6.97 \bullet 10^{-06}$	$1.05 \bullet 10^{-05}$

$$r_1 = \frac{d\left[NO_2^-\right]_t}{dt} = K_{1;560/620°C} \cdot \frac{\left[NO_2^-\right]}{\left[NO_3^-\right]} \tag{7}$$

$$r_2 = \frac{d\left[O^{2-}\right]_t}{dt} = K_{2;560/620°C} \cdot \frac{\left[O^{2-}\right]}{\left[NO_2^-\right]} \tag{8}$$

For this calculation, the change in the nitrite/nitrate ion concentration or the oxide/nitrite ion concentration is plotted over the reaction time. The slope of the resulting fit corresponds to the reaction constant $k_{1/2}$ of the respective reaction in h^{-1}. Fig. 7 exemplarily shows the described procedure for the graphical determination of the reaction constant k_1 on the basis of the reduction from equation (1) using the data obtained in V1 at 620 °C.

The reaction constants k_1 and k_2 obtained from both experiments in this study, converted from h^{-1} to s^{-1}, as well as previously

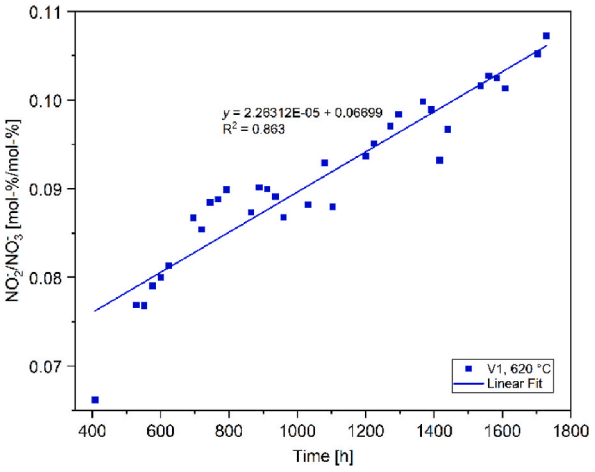

Fig. 7. Nitrite-Nitrate concentrations and resulting graphical determination of the reaction constant k_1 on the basis of the reduction from equation (1) for V1 at 620 °C.

published data from lab scale experiments are summarized in Table 2 [20–22]. For $T = 560$ °C no k_1 could be extracted from the data of this study. V1 was already in an equilibrium due to the added nitrite in the initial salt melt and V2 showed a beginning regeneration, that was disturbed by heating up the system, thus not enough data points are available for the determination of k_1 at 560 °C.

A comparison, shown in Fig. 8, of the reduction rates $k1$ of the first decomposition step according equation (1), with data from laboratory tests published by Sötz et al. (mg-scale and ≤1.5 g-scale) shows that the rate constants in the 100 kg-scale are, significantly lower by four orders of magnitude [21,22]. This difference can be explained by the marked differences in the experimental set-up, applied gas atmospheres and the higher mass transport limitations of anions and gases inside the salt and gas phase of the 100 kg system, despite using a mechanical stirrer in V2. The small lab scale experiments featured very thin molten salt films and removal of developed reactive gases (O_2/NO_x) in a natural convection driven air stream, that lead to a faster decomposition by rapid degassing the formed gases from the bulk. The experiments in this study, performed under semi-closed conditions conserved the gases, developed by the decomposition reactions. This led to an accumulation of oxygen and nitrous gases in the gas atmosphere inside the retort, resulting in a stabilization of the salt melt by shifting the reactions (1) and (2) to the left side, lowering the reduction rate constants k_1.

The rate constants k_2 for the reduction of reaction (2) obtained from the 100 kg-scale experiments of this study are lower by three orders of magnitude at $T = 560$ °C and 4 (V1) as well as 7 (V2) orders of magnitude at $T = 620$ °C compared to the lab scale experiments by Sötz et al. [21,22]. This result can again be explained by the controlled environment of our setup, purging the gas atmosphere with synthetic air (20 vol-% O_2/80 vol-% N_2) at $T = 25$–560 °C and applying the semi-closed configuration at $T = 560$ °C - 620 °C, linked with equilibration of reaction (1) and hence oxide formation did not take place as frequently as in the small scale experiments. The significant reduction of k_2 between V1 and V2 by about three orders of magnitude can be ascribed to the almost achieved chemical equilibrium in V2. Due to the large fluctuations in the measured values for the oxide contend in V2, no definitive statement can be made, whether equilibrium has been fully reached or not. Nonetheless, finding decomposition rates orders of magnitude lower than in the lab-scale is indicative of the chemistry being close to equilibrium conditions.

3.2.4. Regeneration study V3

Regeneration of the decomposed Solar Salt with a purge gas containing 50 % O2 and 2000 ppm NO (rest N_2) was investigated in the final stage of the test campaign. The purge gas was bubbled through the salt melt as schematically shown in Fig. 1 and the compositions of the salt and gas phase were measured and are plotted over time in Fig. 9. In case of a successful regeneration an increase of the nitrate concentration in the salt and a decrease of the oxygen and NO_x content in the gas phase leaving the system are expected [17].

Fig. 9 shows the obtained data of the composition of the molten salt phase and Fig. 10 the composition of the gas phase leaving the system. The salt phase, shows no significant change in the ion concentrations of the salt samples (within the uncertainty limits or the inhomogeneity of the melt). Thus, data of the salt phase do not demonstrate a regeneration mechanism.

The gas analytical measurements of nitrous gases and oxygen are shown in Fig. 10. The oxygen concentration in the purged gas remains either more or less constant, the small decrease during the experiment time of 450 h (≈0.7 vol-%) lies within the uncertainty area of the measurement device. The NO_x concentration directly exhibits a falling trend, that is increasing over the course of the experiment compared to the initial NO_x concentration (2000 ± 80 ppm). A reduction of the volume flow from 1 L/min to 0.5 L/min accompanied by a decrease of gas pressure after 150 h increases the dwelling time of the gas inside the molten salt phase and with that the consumption of the nitrous gases (see Fig. 10 left, duration 170–450 h). By calculating the amount of salt that can be regenerated with the consumed gas according to equations (1) and (2) it becomes clear, that the change in ion concentration from regeneration over the period of 450 h is very low (<0.01 mol-%) compared to the total concentration of the salt and within the inaccuracy of measurement due to inhomogeneity of the extracted samples. For that reason, it is concluded that no regeneration in the salt phase could be detected. The measurement data seem to show that the nitrous gases, despite the high concentration, have not reacted completely (see Fig. 9 left, NO_x concentration always larger than 1400 ppm). Hence, a large part of NO_x entering the vessel leaves the experiment unconsumed. It is possible that either due to the closed operation, the molten salt is already largely saturated with NO_X gas and despites bubbling the gas through the salt melt while stirring the gas-salt contact area still remains too small. Moreover, the temperature of 620 °C is still high enough to counter any regeneration reaction with decomposition. A lower temperature might by more advisable to achieve both rapid and effective regeneration of the molten salt. Therefore, for an active regeneration in the future it is still necessary to identify more suitable process parameters.

4. Conclusion

The conducted experiments demonstrate the feasibility of a 100 kg technical-scale molten salt reactor operated with Solar Salt at 620 °C using a combination of an open configuration purged with synthetic air (25 °C − 560 °C) and a semi-closed system with a maximum overpressure of 20 mbar (560 °C − 620 °C). It has been shown that even a low allowable maximum pressure of a few mbar is sufficient to generate and accumulate the necessary reactive gas atmosphere ($p_{O_2} = 0.5 - 0.6$ atm, 300 ppm NO_x) to stabilize Solar Salt in the reactor at 620 °C over a long period. The total experiment time was more than 4000 h. The data obtained for nitrate and nitrite concentrations are all in the range expected and extrapolated from small-scale studies. The oxide content was higher than expected from 100 g laboratory-scale experiments with similar gas concentrations but appeared to stabilize and remain constant at the end of the study. A comparison of the reaction constants k_1 and k_2 for the reduction of the well-known decomposition reactions shows that larger systems (≥100 kg) behave much slower than the published small-scale laboratory systems, illustrating the high impact of the stabilizing effect of the applied gas phase in contact with the salt, mass transport limiting effects and the resulting slowed diffusion of anions and gases within the molten salt with increasing salt mass.

In addition, first experiments on regeneration of the aged salt by introducing the liquid phase to reactive gases (NO_x, O_2) were

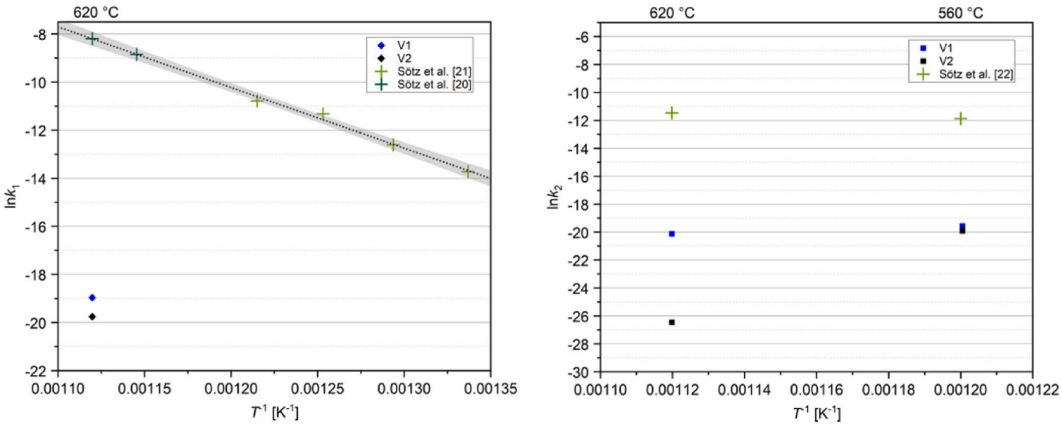

Fig. 8. Arrhenius diagram of the reduction rate constants k_1 for equation (1) (left) and k_2 for equation (2) (right). The rhombus symbols (black, blue) correspond to the rate constants from data of this study at 560 and 620 °C. For comparison, rate constants (green cross symbols), their linear fit (dotted line) and the uncertainty range from previously published lab-scale studies are shown [20–22].

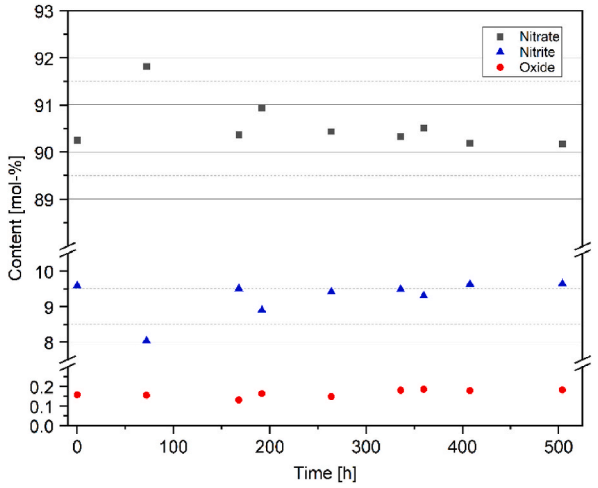

Fig. 9. Anion content of Solar Salt during the regeneration experiment at 620 °C, measured by ion chromatography (NO_2^- blue, NO_3^- black) and titration (O^{2-} red).

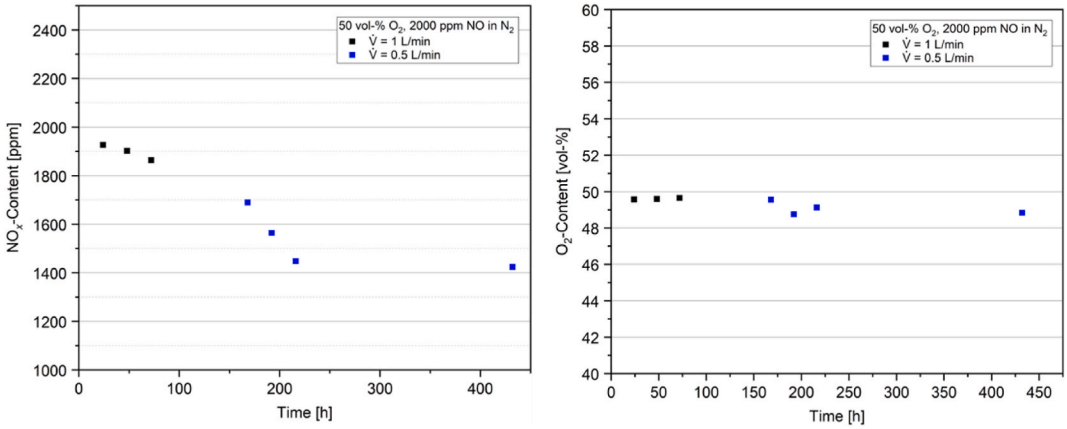

Fig. 10. NO_x ($NO + NO_2$, left) and oxygen (O_2, right) concentrations recorded during the regeneration experiment at 620 °C. At time 150 h, the gas flow was reduced from 1 L/min (black symbols) to 0.5 L/min (blue symbols).

performed and evaluated. It has been shown that, despites NO_x was consumed from the inflowing gas, the gas-salt contact area was to small and the temperature of 620 °C still high enough to counter any regeneration reaction with decomposition. Thus, most of the NO_x left the system without further reaction no relevant regeneration could be observed within the salt composition.

In conclusion, the work demonstrated for the first time the stabilization of Solar Salt at 620 °C in a scale of 100 kg at atmospheric pressure over a duration of about 4000 h. The key to this was a semi-closed gas system that allowed the enrichment of oxygen and nitrogen oxides while maintaining a pressure that can also be used in industrial scale systems. A content of about 50 vol-% oxygen and 300 ppm nitrogen oxides in the gas phase could adequately stabilize the solar salt and prevent decay.

Therefore, it can be said, that 560 °C as the current state-of-the-art temperature is not the upper limit for the future of thermal energy storage hot tanks. CSP plants based on solar salt could therefore reach salt temperatures of around 620 °C if a suitable gas atmosphere is provided. One possible approach could be the application of a semi-closed system.

Data availability statement

Data will be made available on request.

Additional information

No additional information is available for this paper.

CRediT authorship contribution statement

Sebastian Kunkel: Writing – original draft, Visualization, Methodology, Investigation, Data curation, Conceptualization. **Felix Seeliger:** Writing – review & editing, Methodology, Investigation. **Andrea Hanke:** Writing – review & editing, Validation, Investigation. **Thomas Bauer:** Writing – review & editing, Project administration, Funding acquisition. **Alexander Bonk:** Project administration, Funding acquisition, Conceptualization.

Declaration of competing interest

The authors declare the following financial interests/personal relationships which may be considered as potential competing interests: Dr. Sebastian Kunkel reports financial support was provided by German Federal Ministry for Economic Affairs and Climate Action.

Acknowledgement

This work was funded by the German Federal Ministry for Economic Affairs and Climate Action in the project VeNiTe (Ref. No. 03EE5043). We kindly thank in particular Freerk Klasing and Julian Steinbrecher for laboratory work and great expertise in experimental methods.

References

[1] Y. Tian, C.Y. Zhao, A review of solar collectors and thermal energy storage in solar thermal applications, Appl. Energy 104 (2013) 538–553.
[2] M. Sarvghad, S. Delkasar Maher, D. Collard, M. Tassan, G. Will, T.A. Steinberg, Materials compatibility for the next generation of Concentrated Solar Power plants, Energy Storage Mater. 14 (2018) 179–198.
[3] R. Carling, C. Kramer, R. Bradshaw, D. Nissen, S. Goods, R. Mar, J. Munford, M. Karnowsky, R. Biefeld, N. Norem, Molten Nitrate Salt Technology Development Status Report, Sandia National Lab.(SNL-CA), Sandia National Laboratory, Livermore, CA (United States), 1981.
[4] R. Pitz-Paal, Concentrating solar power: still small but learning fast, Nat. Energy 2 (2017), 17095.
[5] M. Roeb, M. Neises, N. Monnerie, C. Sattler, R. Pitz-Paal, Technologies and trends in solar power and fuels, Energy Environ. Sci. 4 (2011) 2503–2511.
[6] M. Romero, A. Steinfeld, Concentrating solar thermal power and thermochemical fuels, Energy Environ. Sci. 5 (2012) 9234–9245.
[7] A. Bonk, S. Sau, N. Uranga, M. Hernaiz, T. Bauer, Advanced heat transfer fluids for direct molten salt line-focusing CSP plants, Prog. Energy Combust. Sci. 67 (2018) 69–87.
[8] M. Durth, C. Prieto, A. Rodríguez-Sánchez, D. Patiño-Rodríguez, L.F. Cabeza, Effects of sodium nitrate concentration on thermophysical properties of solar salts and on the thermal energy storage cost, Sol. Energy 182 (2019) 57–63.
[9] T. Bauer, C. Odenthal, A. Bonk, Molten salt storage for power generation, Chem. Ing. Tech. 93 (2021) 534–546.
[10] R. Roper, M. Harkema, P. Sabharwall, C. Riddle, B. Chisholm, B. Day, P. Marotta, Molten salt for advanced energy applications: a review, Ann. Nucl. Energy 169 (2022), 108924.
[11] T. Bauer, N. Pfleger, D. Laing, W.-D. Steinmann, M. Eck, S. Kaesche, in: F. Lantelme, H. Groult (Eds.), Molten Salts Chemistry, Elsevier, Oxford, 2013, pp. 415–438.
[12] D.A. Nissen, D.E. Meeker, Nitrate/nitrite chemistry in sodium nitrate-potassium nitrate melts, Inorg. Chem. 22 (1983) 716–721.
[13] A. Bonk, C. Martin, M. Braun, T. Bauer, Material investigations on the thermal stability of solar salt and potential filler materials for molten salt storage, AIP Conf. Proc. 1850 (2017), 080008.
[14] H. Li, X. Feng, X. Wang, X. Yang, J. Tang, J. Gong, Impact of temperature on corrosion behavior of austenitic stainless steels in solar salt for CSP application: an electrochemical study, Sol. Energy Mater. Sol. Cell. 239 (2022), 111661.
[15] M. Elbakhshwan, D.H. Lee, M. Anderson, Corrosion resistance of high nickel alloys in solar salt at 600° C for up to 4000 h, Sol. Energy Mater. Sol. Cell. 245 (2022), 111837.
[16] A. Bonk, T. Bauer, Solar Salt - Thermal Property Analysis - Extended Version: Report on Thermo-Physical Prperties of Binary $NaNO_3$-KNO_3 Mixtures in a Range of 55-65 Wt% $NaNO_3$, German Aerospace Center Stuttgart, 2021.
[17] J. Steinbrecher, A. Bonk, V.A. Sötz, T. Bauer, Investigation of regeneration mechanisms of aged solar salt, Materials 14 (2021) 5664.

[18] K. Summers, D. Chidambaram, Corrosion in molten salts for solar thermal power, Electrochem. Soc. Interface 30 (2021) 63.
[19] A. Bonk, M. Braun, V.A. Sötz, T. Bauer, Solar Salt – pushing an old material for energy storage to a new limit, Appl. Energy 262 (2020), 114535.
[20] V.A. Sötz, A. Bonk, J. Steinbrecher, T. Bauer, Defined purge gas composition stabilizes molten nitrate salt - experimental prove and thermodynamic calculations, Sol. Energy 211 (2020) 453–462.
[21] V.A. Sötz, A. Bonk, J. Forstner, T. Bauer, Microkinetics of the reactionNO3-⇌NO2-+0.5 O2in molten sodium nitrate and potassium nitrate salt, Thermochim. Acta (2019) 678.
[22] V.A. Sötz, A. Bonk, T. Bauer, With a view to elevated operating temperatures in thermal energy storage - reaction chemistry of Solar Salt up to 630°C, Sol. Energy Mater. Sol. Cell. 212 (2020), 110577.
[23] D.-S. Li, G. Chen, D. Li, Q. Zheng, P. Gao, L.-L. Zhang, Oxidation resistance of nickel-based superalloy Inconel 600 in air at different temperatures, Rare Met. 40 (2021) 3235–3240.
[24] D. Saber, I.S. Emam, R. Abdel-Karim, High temperature cyclic oxidation of Ni based superalloys at different temperatures in air, J. Alloys Compd. 719 (2017) 133–141.
[25] B.J. Brough, D.H. Kerridge, S.A. Tariq, Molten lithium-potassium nitrate eutectic: the reactions of some compounds of chromium, Inorg. Chim. Acta. 1 (1967) 267–270.
[26] A.K.K. Lee, E.F. Johnson, Stoichiometry and kinetics of the thermal decomposition of molten anhydrous lithium nitrite, Inorg. Chem. 11 (1972) 782–787.
[27] B.D. Bond, P.W.M. Jacobs, The thermal decomposition of sodium nitrate, J. Chem. Soc. Inorg. Phys. Theor. (1966) 1265–1268.